Proceedings of the 4th International Conference on Applied Physics and Mathematical Modeling
DOI: 10.54254/2753-8818/2026.38143

Bingham Fluid Rheology and a Dimensionless Analysis of Wire Cutting in Fresh Cementitious Filaments

Hongyan Yang

Beijing No.4 High School, Beijing, China
hongyan.yang08@outlook.com

Abstract. Bingham fluids combine a finite yield stress with an approximately linear post-yield relation between shear stress and shear rate. This compact model is widely used for pastes, slurries, drilling muds, cementitious materials and other viscoplastic media, yet its apparent simplicity conceals the free-boundary problem created by yielded and unyielded regions. This article reviews the constitutive basis of the Bingham model, analytical results for simple flows, and numerical strategies based on regularization, finite elements and the lattice Boltzmann method. The review emphasizes that yield surfaces are stress-defined rather than material interfaces and that regularization parameters must be checked against mesh and time-step sensitivity. A feasible research object is then developed: transverse wire cutting of a freshly extruded cementitious filament. The wire is treated as a translating cylinder in a low-Reynolds-number yield-stress medium. A dimensionless analysis based on the Bingham number separates viscous-dominated, mixed and yield-dominated cutting regimes, while a transparent resistance scale links yield stress, plastic viscosity, wire diameter and cutting speed. The analysis shows why slower cutting does not necessarily minimize resistance when structural rebuilding raises the yield stress. A combined rheometry, force-measurement and regularized-flow simulation protocol is proposed. The Bingham model is suitable as a baseline for process design, but thixotropy, elasticity, wall slip, particle size and fracture must be added when they control the observed cutting response.

Keywords: Bingham fluid, yield stress, viscoplastic flow, wire cutting, cementitious filament

1. Introduction

Yield-stress materials remain apparently solid under weak loading but flow once a critical stress is exceeded. Bingham introduced a linear post-yield description for this behavior [1]. Later treatments established the model as a useful idealization for suspensions, pastes, foams, waxy oils and cementitious mixtures [2-5]. Its engineering appeal comes from two interpretable parameters: the yield stress τ_0, which controls the onset and spatial extent of flow, and the plastic viscosity μ_p, which controls dissipation after yielding. The same feature that makes the model attractive also makes it difficult: the boundary between yielded and unyielded zones is unknown before the flow solution is obtained.

© 2026 The Authors. This is an open access article distributed under the terms of the Creative Commons Attribution License 4.0 (https://creativecommons.org/licenses/by/4.0/).

DOI: 10.54254/2753-8818/2026.38143

Farina and Fusi [5] provide the mathematical foundation of this review, including yield surfaces, lubrication limits and moving fronts. Tang et al. [6] connect that theory to computation through Papanastasiou-regularized, incompressible LBM benchmarks for channel, expansion and cavity flows. Supporting studies were selected for experimental yield-stress flow, obstacle drag, cement rheometry and extrusion-based additive manufacturing [3, 4, 7-11]. The review is narrative rather than systematic.

The application is a freshly extruded cementitious filament severed transversely by a thin wire, relevant to start-stop deposition and automated finishing. The wire maps onto a cylinder translating through a yield-stress medium [7-9]. The aim is an auditable Bingham baseline that identifies dimensionless controls and clear criteria for adopting a more complex model.

2. Constitutive and mathematical framework

2.1. Ideal Bingham behavior

For simple shear, the ideal constitutive law separates a rigid response from a linear viscous response. Using magnitudes of shear stress τ and shear rate $\dot{\gamma}$, the one-dimensional form is

$$\tau = \tau_0 + \mu \quad \dot{\gamma} \text{ for } \tau > \tau_0; \quad \dot{\gamma} = 0 \text{ for } \tau \leq \tau_0 \tag{1}$$

Below yield, the rate of deformation vanishes in the ideal theory and an unyielded zone may move as a plug. In multiple dimensions, yielding is decided from stress and strain-rate invariants. The contour $|\tau| = \tau 0$ is a stress-defined boundary, not a permanent material interface [3-5].

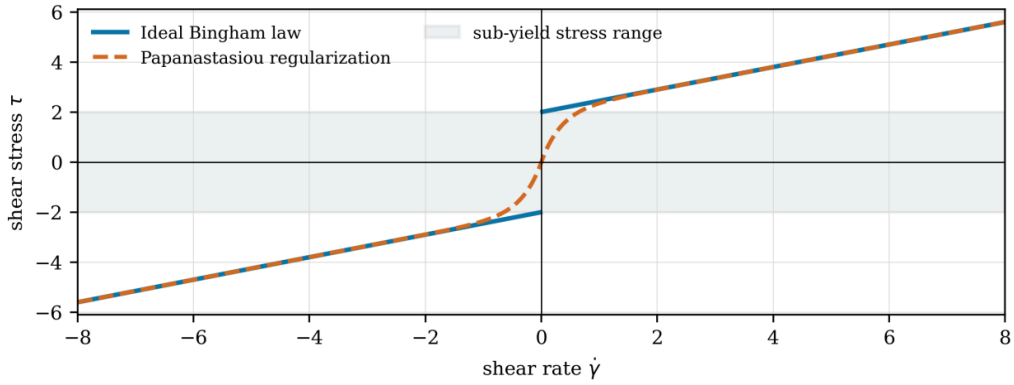


Figure 1. Ideal Bingham response and a smooth Papanastasiou approximation

2.2. Regularization and numerical treatment

The discontinuity at zero shear rate complicates conventional computational fluid dynamics. Papanastasiou [12] replaced the singular apparent viscosity by a smooth exponential expression valid across the whole domain:

$$\tau = \mu \quad \dot{\gamma} + \tau_0 \, [1 - exp(-m\dot{\gamma})] \tag{2}$$

Here m is a stress-growth or regularization parameter. As m increases, the low-shear viscosity rises and the solution approaches the ideal Bingham limit, but an excessively large value produces stiffness and worsens convergence. Tang et al. [6] demonstrate this trade-off in an incompressible

DOI: 10.54254/2753-8818/2026.38143

lattice Boltzmann method (LBM). Their channel-flow profiles agree with analytical solutions, while sudden-expansion and cavity calculations show that increasing the Bingham number enlarges unyielded regions and suppresses recirculation. The work is especially relevant to moving-tool problems because LBM handles complex boundaries efficiently, although force prediction still requires careful boundary and grid treatment.

Finite-element variational methods can retain a sharper yield criterion and adapt the mesh near yield surfaces [7]. Regularized solvers are easier to combine with moving boundaries and free surfaces. In either case, mesh size, time step and m must be converged together; otherwise the computed plug can be a numerical artifact.

Table 1. Numerical representations of Bingham flow

Approach	Principal advantage	Main limitation	Use in cutting analysis
Ideal variational	Sharp yield criterion	Specialized solver; costly moving boundaries	Reference solution for low-Re cases
Bi-viscosity	Simple and robust	Artificial viscosity ratio controls the plug	Rapid sensitivity screening
Papanastasiou	Smooth stress-rate law; broad CFD support	Result depends on m until converged	Preferred moving-wire baseline
Incompressible LBM	Local operations and complex-boundary convenience	Relaxation stability and boundary-force accuracy	Efficient parameter sweep

3. Insights from canonical bingham flows

3.1. Channels lubrication and geometric transitions

In pressure-driven channel flow, low centerline stress creates a plug; a stronger pressure gradient thins it, while larger $\tau 0$ enlarges it. The same pattern appears in complex geometries as thin yielded layers near solid boundaries and weakly deformed cores. Farina and Fusi [5] caution that lubrication approximations can become inconsistent if stresses on the plug boundary are mishandled. Regularization may conceal, rather than resolve, this lubrication paradox [13].

Expansion and cavity flows show that yield stress changes flow topology. Tang et al. [6] found that larger Bn expands unyielded zones and suppresses recirculation. Behind a cutting wire, an almost zero-strain region may therefore be a translating bridge rather than a separated cut; local yielding must be coupled with free-surface separation or material displacement.

3.2. Obstacle motion and drag

Cylinder studies are the closest analogue to wire cutting. Adaptive simulations resolve bounded yielded envelopes and wall effects [7], while slow-motion experiments show that roughness, slip and confinement strongly affect drag [8, 9, 14]. Wire diameter, surface condition, filament size and support-plate distance must therefore be controlled alongside speed.

DOI: 10.54254/2753-8818/2026.38143

The analogy applies only while the wire opens a path mainly by yielding. If a crack advances ahead of the wire, hydrodynamic drag is insufficient and fracture or elastoviscoplastic mechanics are required. High-speed images should determine which mechanism occurs.

4. Wire cutting of a fresh cementitious filament

4.1. Research object and assumptions

The proposed specimen is a fresh filament of diameter Df = 30 mm cut by a d = 2 mm stainless-steel wire moving at speed U. Cementitious extrusion is governed by yield stress, viscosity and time-dependent structuration [10, 11, 15]. The baseline assumes an incompressible, homogeneous Bingham material, no slip on the wire and a stress-free outer surface. Gravity can be neglected when wire transit is short compared with slump.

Cutting is defined here as wire-induced yielding and displacement, not brittle fracture. Carbopol gel can first provide transparent optical validation of the yielded envelope; the cementitious mixture then supplies application-relevant force data.

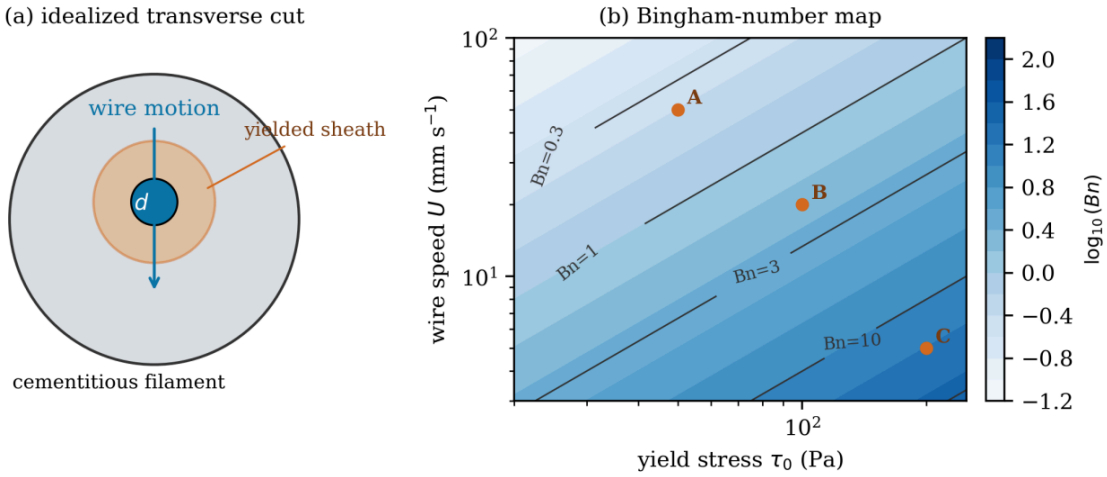


Figure 2. Proposed wire-cutting object and illustrative dimensionless operating map

4.2. Dimensionless process analysis

With the wire diameter as the local length scale, the plastic Reynolds number and Bingham number are

$$\mathrm{Re} = \rho U d/\mu \quad , \quad \mathrm{Bn} = \tau_0\ d/(\mu \quad U) \tag{3}$$

Re compares inertia with viscous stress, whereas Bn compares yield stress with the viscous stress scale μpU/d. When Re $\ll$ 1, the process is creeping and force is governed mainly by Bn, confinement and slip. Bn < 1 indicates that speed-dependent viscous stress is larger than yield stress near the wire; Bn $\approx$ 1 is a mixed regime; and Bn $\gg$ 1 is yield-dominated. A transparent local resistance scale, not a universal drag law, is

$$S = \tau_0\ + \mu \quad U/d, \quad \widehat{F} = S(dDf), \quad \chi y = \tau_0/S = Bn/(1 + Bn) \tag{4}$$

DOI: 10.54254/2753-8818/2026.38143

S evaluates the constitutive stress at the rate U/d, $\hat{F}$ is a projected-area scale, and χ_y is its yield fraction. $\hat{F}$ is not a universal force law: geometry, free-surface evolution, confinement and slip still require simulation or calibration.

Table 2. Illustrative cutting regimes for d = 2 mm Df = 30 mm μp = 5 Pa s and ρ = 2000 kg m−3

Case	τ_0 (Pa)	U (mm s−1)	Re	Bn	χ_y	$\hat{F}$ (N)
A	50	50	0.040	0.40	0.286	0.0105
B	100	20	0.016	2.00	0.667	0.0090
C	200	5	0.004	16.0	0.941	0.0128

Table 2 keeps Re below 0.05 but spans Bn from 0.4 to 16. Case A is viscosity-dominated, Case B is mixed, and Case C is nearly rate-independent. Therefore, slower cutting does not always reduce resistance. In thixotropic paste, additional time can raise τ0 and offset the fall in μpU/d. A moderate Bn is the most plausible operating window for a continuous yielded sheath without excessive viscous drag.

4.3. Proposed computational and experimental protocol

The computation should reproduce channel flow and a cylinder benchmark before adding a free surface. A two-dimensional moving-wire model can use an arbitrary-Lagrangian-Eulerian, immersed-boundary or LBM treatment with Papanastasiou regularization. At least three m values and three near-wire mesh sizes should be tested. Outputs are total force, pressure and shear contributions, yielded-area fraction and any unyielded bridge behind the wire.

The experiment should pair history-controlled rheometry with force measurement. Static τ0 is measured after a fixed rest, then μp from a descending shear-rate ramp [10]. Filaments are cut at controlled ages using multiple wire diameters, speeds and rest times. A load cell records force-displacement, and roughness is documented because slip alters drag [9, 14]. Collapse of F/(μpUDf) against Bn is the primary test of the baseline model.

Predefined rejection criteria include strong cut-to-cut hysteresis, an elastic force overshoot, visible crack propagation or aggregate-scale force oscillations. These observations respectively motivate thixotropic, elastoviscoplastic, fracture or multiphase extensions.

5. Discussion

The literature supports three transferable conclusions: yield stress changes flow topology [3-9, 12]; regularization must be converged rather than treated as a material constant [6, 12, 13]; and obstacle force is sensitive to slip and confinement [8, 9, 14]. Wire cutting is therefore a compact test of yielding, drag, surface deformation and process timing.

The Bingham model is defensible when the post-yield curve is nearly linear over the wire-induced shear-rate range and cutting is fast relative to structural rebuilding. Fresh cement may shear-thin, age, store elastic energy and contain particles comparable with the wire. Its τ0 and μp are therefore protocol-dependent effective parameters and predictions must be limited to the tested process history.

The force scale captures yield-versus-viscous competition but not the drag coefficient. Quantitative design still requires calibration. Its advantage is experimental separation: Cases A-C

DOI: 10.54254/2753-8818/2026.38143

vary Bn fortyfold while keeping inertia negligible, after which confinement H/d and wire roughness can be varied independently.

6. Conclusion

Bingham mechanics describes a material that resists flow below τ0 and dissipates through μp after yield. Unknown yield surfaces remain the central challenge. Channel solutions explain plugs, while regularized finite-element and LBM methods extend the model to transitions, cavities and moving obstacles. Papanastasiou regularization is practical only when m is converged.

Transverse wire cutting of a fresh cementitious filament links this framework to manufacturing. Re and Bn separate creeping viscous, mixed and yield-dominated regimes and show why slower motion need not lower resistance. The proposed workflow combines rheometry, force-displacement data, optical validation and regularized simulation. Bingham behavior is the baseline; thixotropy, elasticity, slip, granular effects and fracture are added only when predefined observations reject it.

References

[1] Bingham, E. C. (1916). An investigation of the laws of plastic flow. *U.S. Bureau of Standards Bulletin, 13*, 309-353.

[2] Bird, R. B., Dai, G. C., & Yarusso, B. J. (1983). The rheology and flow of viscoplastic materials. *Reviews in Chemical Engineering, 1*, 1-70.

[3] Balmforth, N. J., Frigaard, I. A., & Ovarlez, G. (2014). Yielding to stress: Recent developments in viscoplastic fluid mechanics. *Annual Review of Fluid Mechanics, 46*, 121-146. https://doi.org/10.1146/annurev-fluid-010313-141424

[4] Coussot, P. (2014). Yield stress fluid flows: A review of experimental data. *Journal of Non-Newtonian Fluid Mechanics, 211*, 31-49. https://doi.org/10.1016/j.jnnfm.2014.05.006

[5] Farina, A., & Fusi, L. (2018). Viscoplastic fluids: Mathematical modeling and applications. In *Non-Newtonian Fluid Mechanics and Complex Flows*, 229-298. Springer. https://doi.org/10.1007/978-3-319-74796-5_5

[6] Tang, G. H., Wang, S. B., Ye, P. X., & Tao, W. Q. (2011). Bingham fluid simulation with the incompressible lattice Boltzmann model. *Journal of Non-Newtonian Fluid Mechanics, 166*, 145-151. https://doi.org/10.1016/j.jnnfm.2010.11.005

[7] Roquet, N., & Saramito, P. (2003). An adaptive finite element method for Bingham fluid flows around a cylinder. *Computer Methods in Applied Mechanics and Engineering, 192*, 3317-3341. https://doi.org/10.1016/S0045-7825(03)00262-7

[8] Tokpavi, D. L., Magnin, A., & Jay, P. (2008). Very slow flow of Bingham viscoplastic fluid around a circular cylinder. *Journal of Non-Newtonian Fluid Mechanics, 154*, 65-76. https://doi.org/10.1016/j.jnnfm.2008.02.006

[9] Jossic, L., & Magnin, A. (2009). Drag of an isolated cylinder and interactions between two cylinders in yield stress fluids. *Journal of Non-Newtonian Fluid Mechanics, 164*, 9-16. https://doi.org/10.1016/j.jnnfm.2009.07.002

[10] Feys, D., Cepuritis, R., Jacobsen, S., Lesage, K., Secrieru, E., & Yahia, A. (2017). Measuring rheological properties of cement pastes: Most common techniques, procedures and challenges. *RILEM Technical Letters, 2*, 129-135. https://doi.org/10.21809/rilemtechlett.2017.43

[11] Mechtcherine, V., Bos, F. P., Perrot, A., Leal da Silva, W. R., Nerella, V. N., Fataei, S., Wolfs, R. J. M., Sonebi, M., & Roussel, N. (2020). Extrusion-based additive manufacturing with cement-based materials: Production steps, processes, and their underlying physics. *Cement and Concrete Research, 132*, 106037. https://doi.org/10.1016/j.cemconres.2020.106037

[12] Papanastasiou, T. C. (1987). Flows of materials with yield. *Journal of Rheology, 31*(5), 385-404. https://doi.org/10.1122/1.549926

[13] Putz, A., Frigaard, I. A., & Martinez, D. M. (2009). On the lubrication paradox and the use of regularisation methods for lubrication flows. *Journal of Non-Newtonian Fluid Mechanics, 163*, 62-77. https://doi.org/10.1016/j.jnnfm.2009.06.006

[14] Ouattara, Z., Jay, P., Blésès, D., & Magnin, A. (2018). Drag of a cylinder moving near a wall in a yield stress fluid. *AIChE Journal, 64*(11), 4118-4130. https://doi.org/10.1002/aic.16220

[15] Roussel, N., Ovarlez, G., Garrault, S., & Brumaud, C. (2012). The origins of thixotropy of fresh cement pastes. *Cement and Concrete Research, 42*, 148-157. https://doi.org/10.1016/j.cemconres.2011.09.004